Self-Assembly

DOI: 10.1002/anie.201207647

Nonlinear Amplification of a Supramolecular Complex at a Multivalent Interface**

Shu-Han Hsu, M. Deniz Yilmaz, David N. Reinhoudt, Aldrik H. Velders, and Jurriaan Huskens**

Self-assembly leads to reproducible and organized structures that are of interest for applications such as biomembranes,[1] biosensing,[2] and templating.[3,4] As such, self-assembly plays a pivotal and cross-fertiziling role between chemistry and biology, and addresses a range of phenomena such as cooperativity, nonlinear amplification, and error correction. For example, the question of how molecules associated with life, which evolved from an achiral environment, have become homochiral has intrigued scientists for long time, not only owing to their implication for the emergence of life in nature, but also because of their significance to chemical reactions and technical processes.[5,6] Therefore, amplification of chirality is a key to understand the origin of chirality in biomolecules in nature, where such nonlinear amplification has been observed in autocatalytic asymmetric reactions,[7] helical macromolecules,[8–10] peptide assembly,[11–14] template-directed synthesis,[15–17] and supramolecular assemblies.[18–21] In general, nonlinear amplification of a supramolecular complex can provide control in bottom-up fabrication of nanomaterials.[5]

Moreover, nature has selected numerous molecular recognition motifs over billions of years for particular functions, such as oligopeptides for recognition at cell membranes.[22,23] These finest molecular details and intricate noncovalent interactions in biology inspire the learning of the basic molecular engineering principles through the understanding of molecular self-assembly phenomena.[24–28] Owing to the lability of the noncovalent interactions that hold the motifs together, supramolecular entities present the ability to reversibly modify their constitution through exchange and rearrangement of their molecular components; this process eventually can lead to structural amplification.[29,30] The amplification of a given constituent represents a process of self-correction by selection, that is, a process by which the formation of a structure drives the selection of the components that produce the most highly organized and most stable assembly.[31]

We report here a nonlinear amplification process of the complex formation induced and tuned by competition-driven ligand exchange on a multivalent surface. Multivalency describes the interactions that occur here between multivalent receptors and multivalent ligands. Supramolecular, multivalent interactions are of high interest, since multivalency is one of nature's governing principles in for example, protein–carbohydrate interactions, cell recognition,[32,33] as well as a powerful tool for molecular nanostructure fabrication.[34–36] Multivalent interactions at interfaces, e.g., at cell membranes,[37] at lipid membranes,[38,39] or at self-assembled monolayer (SAM) model systems,[40,41] are particularly important, since such interfaces, when functionalized with monovalent receptors or ligands can act as multivalent systems.[35] Multivalent binding events have collective properties different from monovalent interactions; these properties lead to higher binding affinities between the interacting functionalities.

The used cyclodextrin (CD)-based monolayers, so-called molecular printboards, serving as a multivalent receptor platform for multivalent ligands, permit the supramolecular positioning of reversible self-assembled patterns, offering additional benefits regarding control over molecular orientation and stability of binding. The reversible nature of host–guest interactions offers the possibility of self-correction and tunability by changing the conditions, where the immobilized host monolayer allows the variation of environmental conditions, such as competition by a host in solution or change of the polarity of the solution.[36,42] Therefore, a reversible system will operate under thermodynamic control, and will ultimately favor formation of the most stable structures and assure that imperfections are corrected.

Previously, we have employed the antenna and EDTA–Eu^{3+} ligand-based host–guest interactions on the molecular printboard to form a complex that signals its own correct assembly by exhibiting sensitized lanthanide luminescence (Figure 1).[43] In the present study, the intrinsic signaling property of this complex is used to study the self-assembly-driven amplification process of the complex formation induced by competition-driven ligand exchange on a multivalent surface. The antenna-sensitized Eu^{3+} luminescence at the molecular printboards allows assessment of the stoichi-

[*] Dr. S.-H. Hsu,[§] Dr. M. D. Yilmaz, Prof. Dr. D. N. Reinhoudt, Prof. Dr. A. H. Velders,[+] Prof. Dr. J. Huskens
Molecular NanoFabrication and Supramolecular Chemistry & Technology groups, MESA+ Institute for Nanotechnology
University of Twente
P.O. Box 217, 7500 AE Enschede (The Netherlands)
E-mail: aldrik.velders@wur.nl
j.huskens@utwente.nl

[+] Current address: Bio-device NanoTechnology
Wageningen University (The Netherlands)

[§] Current address: National Nano Device Laboratories
Hsinchu 300 (Taiwan)

[**] This work was supported by NanoNed, the nanotechnology program of the Dutch Ministry of Economic Affairs (Grant TMM 6976), and by the Council for Chemical Sciences of the Netherlands Organization for Scientific Research (NWO-CW; grants 700.55.029 and 700.58.443).

Supporting information for this article is available on the WWW under http://dx.doi.org/10.1002/anie.201207647.

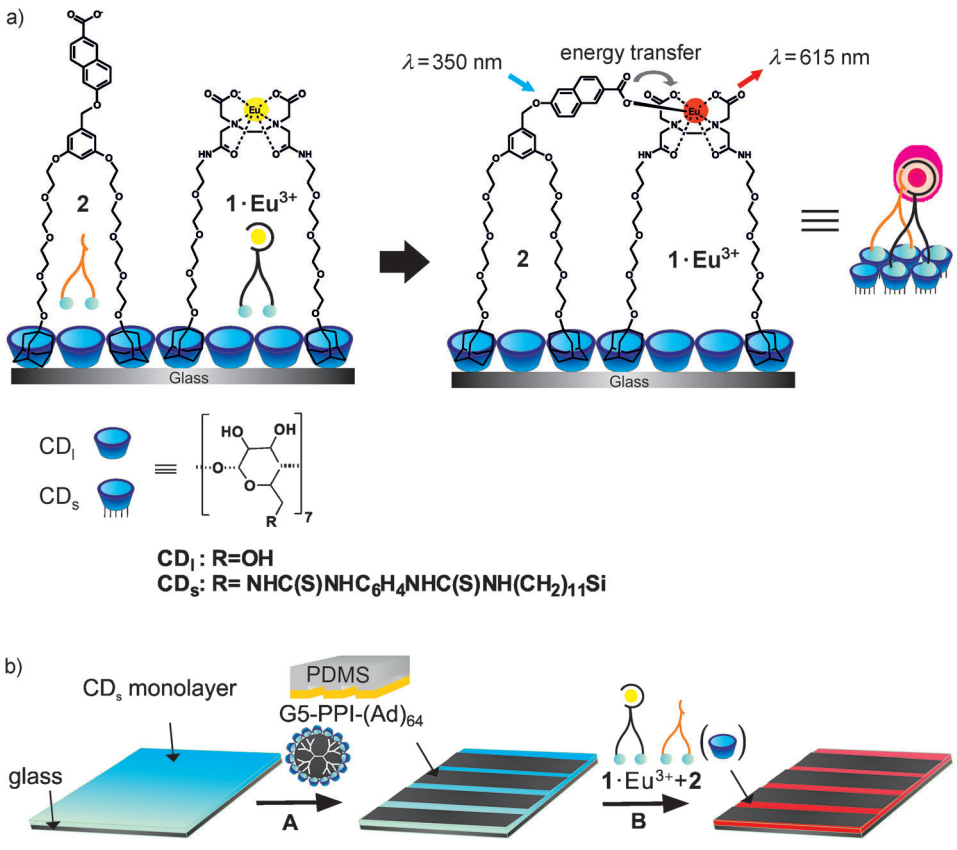

Figure 1. Molecular structure of the target complex on a CD monolayer and representations of sample preparation procedures: a) the complexation of **2** and **1**·Eu^{3+} on a CD monolayer and the occurrence of sensitized luminescence upon coordination of **2** to the Eu^{3+} center, b) a CD monolayer is patterned with G5-PPI-$(Ad)_{64}$ dendrimers by μCP (A), followed by drop-casting a mixture of **1**·Eu^{3+} and **2**, with or without CD_l present in solution, and equilibration for an hour (B). G5-PPI = fifth-generation poly(propylene imine) dendrimer; PDMS = poly(dimethylsiloxane).

ometry of the complex under host-induced binding competition and a quantitative estimation of the surface composition and of the complex binding strength. The data are supported by thermodynamic modeling to explain the observed behavior.

Five different building blocks were used to study multivalent, orthogonal complexation at a CD monolayer (Figure 1a): an EDTA-based ligand **1** for binding a Eu^{3+} ion, the Eu^{3+} ion, a naphthalene-based antenna molecule **2** with a carboxylate group for coordination to the Eu^{3+} ion, cyclodextrin in solution (CD_l), and a cyclodextrin (CD_s) monolayer, which functions as the receptor surface. The EDTA ligand and the antenna molecule are equipped with adamantyl (Ad) groups for noncovalent interaction with the CD monolayer. The CD monolayer is used to immobilize both the sensitizer **2** and the Eu^{3+} complex **1**·Eu^{3+}, thus enforcing the close proximity of the molecules and facilitating sensitized lanthanide luminescence owing to efficient energy transfer.

Microcontact printing (μCP) of G5-PPI-$(Ad)_{64}$ onto the CD monolayers was used to generate surface patterns—as background for good image contrast and quantitative intensity assessment—on the receptor surface.[44] This leaves the unpatterned areas accessible for immobilization of **1**·Eu^{3+} and **2** from solution (Figure 1b). To study the complexation of **1**·Eu^{3+} and **2** on the surface, solution mixtures of different molar ratios of **1**·Eu^{3+} and **2** were incubated over CD monolayers, which were prepatterned with G5-PPI-$(Ad)_{64}$ dendrimers.

The experiments were performed without (kinetically controlled assembly) or with adding CD_l (thermodynamically controlled assembly) as a competing host (Figure 2). In the former case, filling of the surface is expected to be rapid (Figure 2a) and cannot be followed by exchange, because the divalent ligands are assembled in a kinetically stable fashion.[45,46] On the other hand, the addition of CD_l promotes the desorption of immobilized molecules, and hence the adsorption of molecules from solution to reach the stable formation of the complex with the highest valency, that is, the tetravalent complex (Figure 2b). The latter provides the thermodynamic driving force for the exchange process.

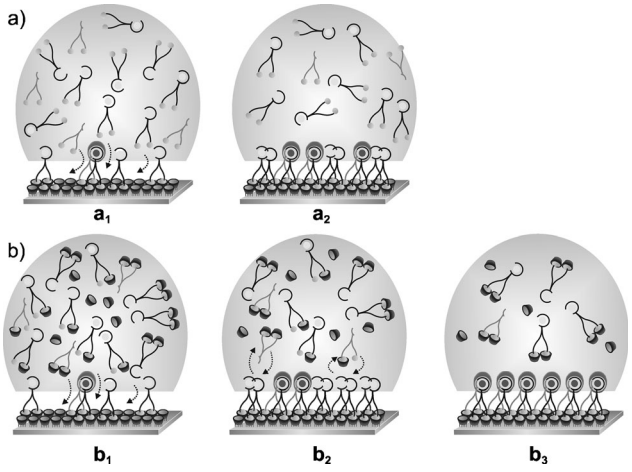

Figure 2. Schematic representation of two assembly procedures of **1**·Eu^{3+} and **2** onto CD monolayers: without (kinetically controlled assembly, (a)) or with (thermodynamically controlled assembly, (b)) CD_l present in the solution mixtures: a) By rapid filling of the empty CD_s surface (a_1) in the absence of CD_l, the two different adamantyl-functionalized ligands are assembled on the surface, with the ratio linearly corresponding to the solution ratio (a_2); b) after the rapid filling of the empty CD surface (b_1) leading to a filled surface (b_2), the self-organization by dynamic exchange is promoted by the presence of CD_l, thus promoting the formation of the stable tetravalent complex (**1**·Eu^{3+}·**2**) under thermodynamic equilibrium (b_3).

Solutions of different molar ratios of **1**·Eu^{3+} and **2** without CD_l present (kinetically controlled assembly) were prepared to study the resulting surface composition of the components and to provide a reference point for the experiments performed under thermodynamic control. Solution mixtures of **1**·Eu^{3+} and **2** (the fraction of **2** is set to 0%, 20%, 40%, 50%, 60%, 80%, and 100%) were incubated over G5-PPI-$(Ad)_{64}$-printed CD monolayers for one hour, and were imaged by fluorescence microscopy with two different filter sets R and B.[30]

The fluorescence images and corresponding intensity profiles of **1**·Eu^{3+} and **2** (Figure S2 in the Supporting Information) as a function of the fraction of **2** in solution show: 1) the quenching of antenna emission in accordance with energy transfer to the Eu^{3+} and 2) the optimal sensitized emission at a 1:1 ratio of **1**·Eu^{3+} and **2**. This stoichiometry relation is consistent with the stoichiometry obtained by μCP of different mixtures of **1**·Eu^{3+} and **2**.[43] This result clearly demonstrates that the assembly of surface species in the absence of CD_l is linearly dependent on the solution composition (Figure 3a).

Following procedure (b) in Figure 2, CD monolayers with dendrimer patterns were incubated in solutions of different molar ratios of **1**·Eu^{3+} and **2** in the presence of CD_l (thermodynamically controlled assembly) to study the effect of competition by CD_l on the degree of formation of **1**·Eu^{3+}·**2**. Therefore, first, solution mixtures of **1**·Eu^{3+} and **2** were prepared, for which the fractions of **2** were set to 0%, 1%, 5%, 10%, 20%, 40%, 50%, 60%, 80%, 90%, 95%, 99%, and 100% with CD_l (200 μM) present as well. Consecutively, these solution mixtures were incubated over G5-PPI-$(Ad)_{64}$-printed CD monolayers for one hour and the samples were imaged by fluorescence microscopy with both filters R and B (Figure S3 in the Supporting Information).

When adding CD_l (200 μM) to the solution mixtures of **1**·Eu^{3+} and **2**, the complex formation of **1**·Eu^{3+}·**2** on the surface shows a highly nonlinear dependence on the solution ratio (Figure 3b and Figure S3 in the Supporting Information). At fractions of **2** in the solution mixtures ranging from 10–90%, the fluorescence intensities of both the Eu^{3+} and the antenna **2** indicate a 1:1 ratio of **1**·Eu^{3+} and **2** at the surface, since these intensities are equal to the intensities obtained for a 1:1 mixture without equilibration (Figure 3a). These results infer that the formation of **1**·Eu^{3+}·**2** constitutes a strong thermodynamic driving force for establishing a 1:1 composition at the surface. Kinetically, this equilibrium is established by the competition induced by CD_l, which accelerates desorption of the noncoordinated divalent ligands **1**·Eu^{3+} and **2** and thus promotes exchange of the excess, uncoordinated major component from the surface for the minor component.

For the solution mixtures with fractions of **2** below 10% and above 90%, less Eu^{3+} fluorescence intensity was observed with concomitant variations in the intensity of **2**. These data points indicate the establishment of equilibrium between the statistically preferred adsorption of the major component versus the complexation-driven adsorption of the minor component.

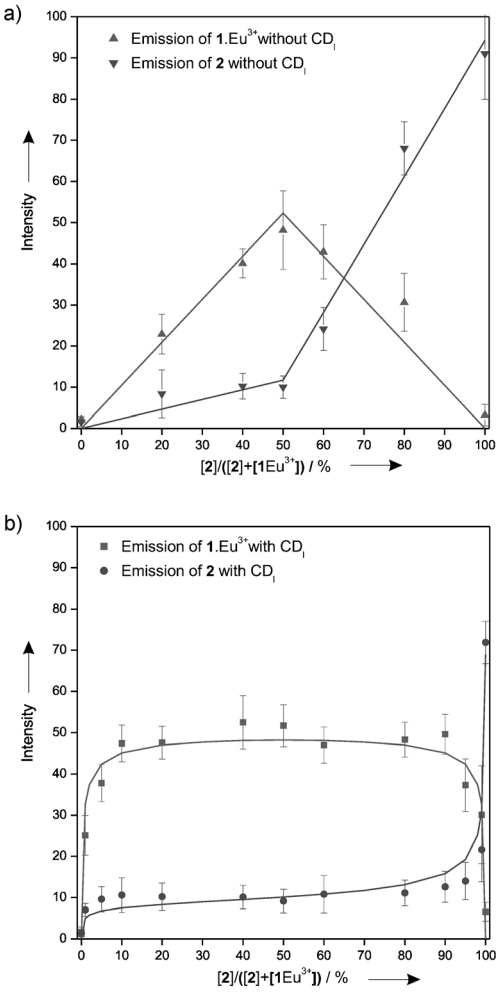

Figure 3. Fluorescence microscopy data of the kinetically and thermodynamically controlled assembly processes: 10 μm lines of G5-PPI-$(Ad)_{64}$ were printed on a CD monolayer and subsequently incubated with solution mixtures of different ratios of **1**·Eu^{3+} and **2** without (a) adding CD_l, and with (b) CD_l (200 μM) by monitoring the emission of Eu^{3+} (R filter) and of **2** (B filter), as shown in Figures S2 and S3 in the Supporting Information. The fluorescence intensities of **1**·Eu^{3+} and **2**, obtained from solution assembly, are shown as a function of the solution composition. Solid curves indicate linear fits (a) and the corresponding fits to the multivalent, sequential binding model (b).

To increase the understanding of the nonlinear amplification of **1**·Eu^{3+}·**2** at the CD monolayer in the presence of CD_l under equilibrium conditions, the complex formation of **1**·Eu^{3+}·**2** was modeled by calculating all surface species concentrations and the concomitant fluorescence intensities as a function of the solution composition while varying the binding constant, K_{AE} of the coordination of the carboxylate group of **2** to the Eu^{3+} center of **1**·Eu^{3+} (Figure S4 in the Supporting Information). The thermodynamic model treats the binding of multivalent ligands to the CD surface as independent binding events, both for inter- and intramolecular binding events (Figure 4a). Because each ligand **1**·Eu^{3+} and **2** can bind to the CD monolayer in a divalent fashion, the maximum coverage of **1**·Eu^{3+} and **2** is only half of the coverage of the CD monolayer, where the monovalent binding of ligands is ignored owing to their lower association

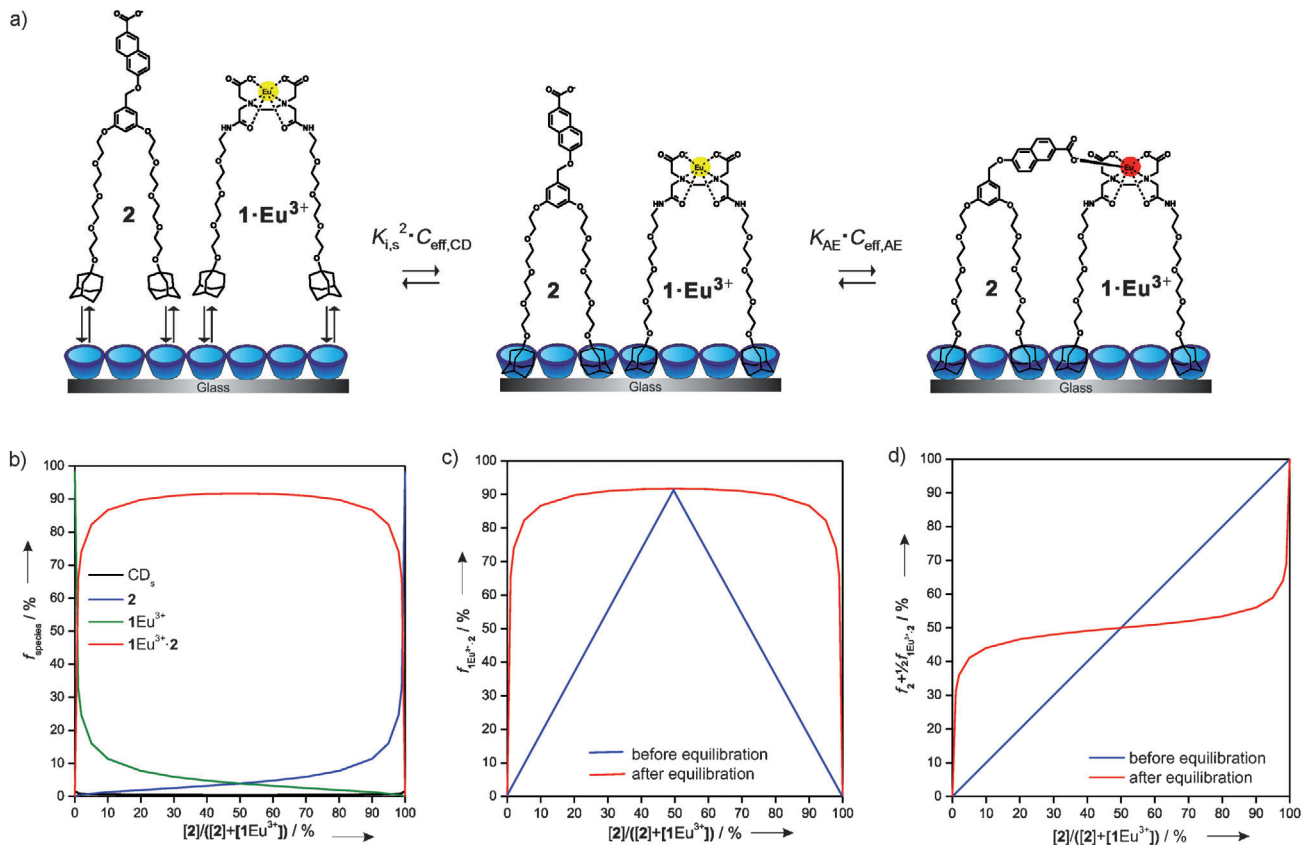

Figure 4. Thermodynamic modeling: a) Schematic representation of solution and surface species of **1**·Eu^{3+} and **2** with two sequential binding events at a CD monolayer: the multivalent binding of **1**·Eu^{3+} and **2** to the CD monolayer is accompanied by an effective concentration term ($C_{eff,CD}$). Coordinative binding: the association constant (K_{AE}) between **1**·Eu^{3+} and **2** is enhanced with an effective concentration term ($C_{eff,AE}$). b) Speciation of divalently bound **1**·Eu^{3+}, divalently bound **2**, tetravalently bound **1**·Eu^{3+}·**2**, and uncomplexed CD_s present at CD monolayers simulated as a function of solution fraction of **2** ($K_{AE} = 6 \times 10^3\ M^{-1}$, $[CD_l] = 200\ \mu M$). c) Surface fraction of **1**·Eu^{3+}·**2** vs. the solution fraction of **2** before (Figure 2 b-b_2) and after (Figure 2 b-b_3) CD equilibration. The curve after equilibration (red) is obtained using the thermodynamic model, whereas the lines before equilibration (blue) correspond to formation of **1**·Eu^{3+}·**2** from **1**·Eu^{3+} and **2**, assuming that their surface ratio is identical to the solution fraction from which they are assembled. d) Surface fraction of **2** (including those of free **2** and **1**·Eu^{3+}·**2**) vs. the solution fraction of **2** before and after CD equilibration.

constants to the CD surface. The model employs binding constants for interaction of an adamantyl group to a CD cavity ($5 \times 10^4\ M^{-1}$), and the 1:1 interaction (K_{AE}) of the antenna carboxylate group with the Eu^{3+} center. The intramolecular binding events are associated with an effective-concentration parameter,[47] which is set to be fourfold lower for the coordination of **2** to **1**·Eu^{3+} than for binding of the divalent ligands to the CD surface, because of the tetravalent nature of the **1**·Eu^{3+}·**2** complex. The modeled fluorescence intensities were obtained by relating these to the fractions of unbound and bound **1**·Eu^{3+} and **2**, assuming fixed values for the emission of **2**, **1**·Eu^{3+}, and the complex **1**·Eu^{3+}·**2**. These values were optimized in the procedure.

Within this model, the fluorescence intensity of antenna **2** increases linearly with the fraction of **2** in solution in the absence of binding ($K_{AE} = 0$), thus indicating that no energy transfer to Eu^{3+} occurs (Figure S5a in the Supporting Information). Upon increase of the binding constant, the antenna emission shows a nonlinear dependence with respect to the solution fraction of **2** because of the simultaneous effects of changing surface composition and fluorescence quenching, both owing to the binding of **2** to **1**·Eu^{3+}. The emission intensity at a value of approximately 10 reflects the remaining intensity of **2** after energy transfer to the Eu^{3+} center upon 1:1 complex formation. At higher binding constants, the intensity plateau becomes more flat and more extended, thereby reflecting a 1:1 surface composition of **1**·Eu^{3+} and **2** at this plateau.

The Eu^{3+} emission versus the solution composition at different binding constants is shown in Figure S5b in the Supporting Information. Overall, the trend of Eu^{3+} emission is similar. Over 90% of the maximum Eu^{3+} emission is reached for $K_{AE} > 10^4\ M^{-1}$, and the plateau where this maximal intensity is reached widens from 50%/50% solution composition to more deviating fractions at higher K_{AE} values in accordance with stabilization and thus amplification of the **1**·Eu^{3+}·**2** complex.

Subsequently, the experimental curves at 200 μM CD_l (Figure 3b) were fitted to the model. The calculated binding constant is $K_{AE} = 6 \times 10^3\ M^{-1}$, which agrees well with the lower limit ($10^3\ M^{-1}$) estimated previously[43] for the assembly to the CD monolayer by μCP.

Figure 4b depicts the simulated speciation of the different components present at the CD surface when using the thermodynamic model in the presence of CD_l at 200 μM and $K_{AE} = 6 \times 10^3\ M^{-1}$. At very low fractions of **2** in solution, **1**·Eu^{3+} is the predominant species at the surface, as it is also in solution (Figure 4b). Upon increase of the solution fraction of **2**, this surface species is rapidly replaced by **1**·Eu^{3+}·**2**. At intermediate fractions between 10% and 90%, **1**·Eu^{3+}·**2** is the major species with a coverage of about 90%. Similarly, at high fractions of **2**, antenna **2** becomes the dominant species present at the CD monolayer. At all fractions of **2**, more than 99% of CD_s is involved in host–guest binding.

The surface coverage of **1**·Eu^{3+}·**2** is plotted versus the solution fraction of **2** in Figure 4c as well (red line), together with the hypothetical case in which the surface is filled with **1**·Eu^{3+} and **2** in the same ratio as present in solution but without subsequent ligand exchange (blue line). The latter very closely resembles the experimental case in the absence of CD_l (Figure 3a). The comparison of these two graphs (Figure 4c) clearly emphasizes the nonlinear amplification of **1**·Eu^{3+}·**2** in case of equilibration; the amplification is induced by CD_l and driven by complex formation between **1**·Eu^{3+} and **2** (Figure 3b). The total fraction of antenna **2** (the sum of the fractions of noncoordinated **2** and of **2** complexed in **1**·Eu^{3+}·**2**) is plotted versus the solution fraction of **2** in Figure 4d. Before equilibration, the surface fraction of **2** is equal to the fraction of **2** in solution. After equilibration, the value of the fraction of **2** on the surface approaches 50% owing to the CD_l-driven formation of **1**·Eu^{3+}·**2**, regardless of the solution fraction of **2**. The plot clearly demonstrates the nonlinear dependence of the surface percentage of **2** on the solution composition.

In conclusion, multivalent interactions at interfaces constitute a complex phenomenon governed by a range of parameters. Here, the multivalent binding of a supramolecular complex at a multivalent host surface, by combining the orthogonal cyclodextrin host-guest and lanthanide-ligand coordination motifs, is described and is used to monitor the molecular binding events. Therefore, the self-correction/self-organization process through host–guest interaction offered by guest-induced competition is reported by the intrinsic signaling property of the sensitized Eu^{3+} emission on the immobilized host monolayer. We successfully explored the ability to vary interactions systematically in a controlled manner at interfaces by adding a competing host. The formation of the **1**·Eu^{3+}·**2** complex has been observed to be linearly dependent on the solution composition in the absence of cyclodextrin, whereas strong nonlinear amplification has been observed under cyclodextrin-promoted thermodynamic equilibrium. Such orthogonal motifs, like cyclodextrin–adamantyl (host–guest) and lanthanide–ligand (coordination), can lead to higher stoichiometries, increased specificity, and more-complex architectures, where the desorption by competition with a host in solution is progressively more difficult owing to increasing numbers of interactions. These results have revealed new and surprising characteristics of multivalent interactions at interfaces. The model described here gives an insight into how multiple, independent interactions provide a collective selection mechanism, where the molecular-level exchange events can be self-reported and provide the evidence for molecular cooperativity, self-recognition, and self-selection on the surface.

Received: September 21, 2012
Published online: November 20, 2012

Keywords: cyclodextrins · multivalency · nonlinear processes · self-assembly · thermodynamic control

[1] M. N. Jones, D. Chapman, *Monolayers and Biomembranes*, Wiley-Liss, New York, **1995**.
[2] S. Kiyonaka, K. Sada, I. Yoshimura, S. Shinkai, N. Kato, I. Hamachi, *Nat. Mater.* **2004**, *3*, 58.
[3] M. Reches, E. Gazit, *Science* **2003**, *300*, 625.
[4] J. Aizenberg, A. J. Black, G. M. Whitesides, *Nature* **1999**, *398*, 495.
[5] R. J. Williams, A. M. Smith, R. Collins, N. Hodson, A. K. Das, R. V. Ulijn, *Nat. Nanotechnol.* **2009**, *4*, 19.
[6] J. L. Bada, *Nature* **1995**, *374*, 594.
[7] C. Girard, H. B. Kagan, *Angew. Chem.* **1998**, *110*, 3088; *Angew. Chem. Int. Ed.* **1998**, *37*, 2922.
[8] M. M. Green, M. P. Reidy, R. J. Johnson, G. Darling, D. J. Oleary, G. Willson, *J. Am. Chem. Soc.* **1989**, *111*, 6452.
[9] M. M. Green, N. C. Peterson, T. Sato, A. Teramoto, R. Cook, S. Lifson, *Science* **1995**, *268*, 1860.
[10] J. Cornelissen, M. Fischer, N. Sommerdijk, R. J. M. Nolte, *Science* **1998**, *280*, 1427.
[11] M. A. Case, G. L. McLendon, *J. Am. Chem. Soc.* **2000**, *122*, 8089.
[12] A. Aggeli, M. Bell, N. Boden, J. N. Keen, P. F. Knowles, T. C. B. McLeish, M. Pitkeathly, S. E. Radford, *Nature* **1997**, *386*, 259.
[13] J. E. Rothman, J. Lenard, *Science* **1977**, *195*, 743.
[14] L. E. R. O'Leary, J. A. Fallas, E. L. Bakota, M. K. Kang, J. D. Hartgerink, *Nat. Chem.* **2011**, *3*, 821.
[15] M. C. Calama, P. Timmerman, D. N. Reinhoudt, *Angew. Chem.* **2000**, *112*, 771; *Angew. Chem. Int. Ed.* **2000**, *39*, 755.
[16] Y. Krishnan-Ghosh, S. Balasubramanian, *Angew. Chem.* **2003**, *115*, 2221; *Angew. Chem. Int. Ed.* **2003**, *42*, 2171.
[17] M. Yoshizawa, J. K. Klosterman, M. Fujita, *Angew. Chem.* **2009**, *121*, 3470; *Angew. Chem. Int. Ed.* **2009**, *48*, 3418.
[18] E. Yashima, K. Maeda, Y. Okamoto, *Nature* **1999**, *399*, 449.
[19] V. Percec, A. E. Dulcey, V. S. K. Balagurusamy, Y. Miura, J. Smidrkal, M. Peterca, S. Nummelin, U. Edlund, S. D. Hudson, P. A. Heiney, D. A. Hu, S. N. Magonov, S. A. Vinogradov, *Nature* **2004**, *430*, 764.
[20] L. J. Prins, J. Huskens, F. de Jong, P. Timmerman, D. N. Reinhoudt, *Nature* **1999**, *398*, 498.
[21] N. Sreenivasachary, J.-M. Lehn, *Proc. Natl. Acad. Sci. USA* **2005**, *102*, 5938.
[22] S. G. Zhang, T. Holmes, C. Lockshin, A. Rich, *Proc. Natl. Acad. Sci. USA* **1993**, *90*, 3334.
[23] G. A. Silva, C. Czeisler, K. L. Niece, E. Beniash, D. A. Harrington, J. A. Kessler, S. I. Stupp, *Science* **2004**, *303*, 1352.
[24] J. S. Lindsey, *New J. Chem.* **1991**, *15*, 153.
[25] G. M. Whitesides, B. Grzybowski, *Science* **2002**, *295*, 2418.
[26] G. M. Whitesides, J. P. Mathias, C. T. Seto, *Science* **1991**, *254*, 1312.
[27] D. N. Reinhoudt, M. Crego-Calama, *Science* **2002**, *295*, 2403.
[28] E. Gazit, *Nat. Chem.* **2010**, *2*, 1010.
[29] J. M. Lehn, *Science* **2002**, *295*, 2400.
[30] S. Mann, *Nat. Mater.* **2009**, *8*, 781.
[31] J. M. Lehn, *Proc. Natl. Acad. Sci. USA* **2002**, *99*, 4763.
[32] M. Mammen, S. K. Choi, G. M. Whitesides, *Angew. Chem.* **1998**, *110*, 2908; *Angew. Chem. Int. Ed.* **1998**, *37*, 2754.
[33] L. L. Kiessling, J. E. Gestwicki, L. E. Strong, *Angew. Chem.* **2006**, *118*, 2408; *Angew. Chem. Int. Ed.* **2006**, *45*, 2348.

[34] A. Mulder, J. Huskens, D. N. Reinhoudt, *Org. Biomol. Chem.* **2004**, *2*, 3409.
[35] J. Huskens, *Curr. Opin. Chem. Biol.* **2006**, *10*, 537.
[36] M. J. W. Ludden, D. N. Reinhoudt, J. Huskens, *Chem. Soc. Rev.* **2006**, *35*, 1122.
[37] J. E. Gestwicki, L. L. Kiessling, *Nature* **2002**, *415*, 81.
[38] M. L. Pisarchick, N. L. Thompson, *Biophys. J.* **1990**, *57*, A292.
[39] E. L. Doyle, C. A. Hunter, H. C. Phillips, S. J. Webb, N. H. Williams, *J. Am. Chem. Soc.* **2003**, *125*, 4593.
[40] N. Horan, L. Yan, H. Isobe, G. M. Whitesides, D. Kahne, *Proc. Natl. Acad. Sci. USA* **1999**, *96*, 11782.
[41] S. J. Metallo, R. S. Kane, R. E. Holmlin, G. M. Whitesides, *J. Am. Chem. Soc.* **2003**, *125*, 4534.
[42] A. Mulder, S. Onclin, M. Peter, J. P. Hoogenboom, H. Beijleveld, J. ter Maat, M. F. Garcia-Parajo, B. J. Ravoo, J. Huskens, N. F. van Hulst, D. N. Reinhoudt, *Small* **2005**, *1*, 242.
[43] S. H. Hsu, M. D. Yilmaz, C. Blum, V. Subramaniam, D. N. Reinhoudt, A. H. Velders, J. Huskens, *J. Am. Chem. Soc.* **2009**, *131*, 12567.
[44] S. Onclin, J. Huskens, B. J. Ravoo, D. N. Reinhoudt, *Small* **2005**, *1*, 852.
[45] A. Mulder, T. Auletta, A. Sartori, S. Del Ciotto, A. Casnati, R. Ungaro, J. Huskens, D. N. Reinhoudt, *J. Am. Chem. Soc.* **2004**, *126*, 6627.
[46] T. Auletta, B. Dordi, A. Mulder, A. Sartori, S. Onclin, C. M. Bruinink, M. Peter, C. A. Nijhuis, H. Beijleveld, H. Schönherr, G. J. Vancso, A. Casnati, R. Ungaro, B. J. Ravoo, J. Huskens, D. N. Reinhoudt, *Angew. Chem.* **2004**, *116*, 373; *Angew. Chem. Int. Ed.* **2004**, *43*, 369.
[47] J. Huskens, A. Mulder, T. Auletta, C. A. Nijhuis, M. J. W. Ludden, D. N. Reinhoudt, *J. Am. Chem. Soc.* **2004**, *126*, 6784.

